Computer Simulation Studies of a Square-Well Fluid in a Slit Pore. Spreading Pressure and Vapor-Liquid Phase Equilibria Using the Virtual-Parameter-Variation Method

ARTICLE *in* THE JOURNAL OF CHEMICAL PHYSICS · FEBRUARY 2001

Impact Factor: 2.95 · DOI: 10.1063/1.481072 · Source: CiteSeer

2 AUTHORS, INCLUDING:

William R Smith
University of Guelph
182 PUBLICATIONS **3,203** CITATIONS

SEE PROFILE

J. Chem. Phys., in press (2000); accepted Dec. 13, 1999

Computer Simulation Studies of a Square-Well Fluid in a Slit Pore. Spreading Pressure and Vapor-Liquid Phase Equilibria Using the Virtual-Parameter-Variation Method

Horst L. Vörtler

Department of Molecular Dynamics and Computer Simulation

Institute of Theoretical Physics

University of Leipzig

Augustusplatz 9-11, 04109 Leipzig, Germany

and

William R. Smith

Department of Mathematics and Statistics, and School of Engineering

College of Physical and Engineering Science

University of Guelph

Guelph, Ontario, Canada N1G2W1

Abstract

We study model square-well fluids with well-width parameter $\lambda = 1.5$ confined to hard planar slits. We derive a general computer simulation method for numerically calculating an arbitrary first derivative of the canonical ensemble partition function with respect to a simulation parameter, which we call the Virtual-Parameter-Variation method. Two special cases of this approach are the Widom test-particle insertion method for calculating the excess chemical potential, and a method for calculating the pressure due to Eppenga and Frenkel [Molec. Phys. **52**, 52, 1303 (1984)]. We use this approach to calculate the volume derivative parallel to the slit walls of the Helmholtz free energy in an (NVT) Monte Carlo simulation, and show that this spreading pressure is numerically consistent with the thermodynamic pressure obtained by integration of the Gibbs-Duhem equation using the simulated chemical potentials of the confined fluid as a function density. We obtain new simulation results for the spreading pressure and the phase equilibrium properties of the confined square-well fluid, and we also estimate its critical point properties, observing a decrease of the critical temperature in comparison to the bulk fluid.

1 Introduction

The study of inhomogeneous fluid models by statistical mechanical methods is important in providing molecular-level understanding of a wide range of experimental surface and interfacial phenomena, such as adsorption and capillary condensation of fluids, examples of which include fluids interacting with biologically active surfaces (membranes) and fluids confined in microporous media (*e.g.*, zeolites). A number of inhomogeneous fluid models have previously been studied by integral equation[1, 2, 3, 4, 5, 6] and computer simulation[7, 9, 8, 10, 11, 12, 13] methods (for a review of work prior to 1990, see Evans[14]). For an inhomogeneous fluid, although calculation of the internal energy and of the chemical potential may be carried out using methods analogous to those used for the bulk fluids, the calculation of the appropriate pressure is not straightforward, since it is not directionally homogeneous. One pressure of interest is a *thermodynamic* pressure, which may in principle be obtained indirectly by integrating the adsorption isotherm using an appropriate Gibbs-Duhem equation. For fluids confined to a slit-like pore, this pressure is the "spreading pressure", Π, the average mechanical pressure parallel to the slit walls[15].

Calculations of phase equilibria for particular fluid models in a slit-like pore[12] and in a cylindrical pore[7] have been carried out employing the constraint of equality of Π for each phase. In the latter case, the Gibbs Ensemble method[7, 16] was used, which does not require the explicit numerical calculation of Π, and the former study implemented a numerical solution of the phase equilibrium conditions using simulations in the so-called *isotension* ensemble. To our knowledge, no numerical calculations of Π itself have been performed previously.

In this paper, we calculate Π and the vapor-liquid phase equilibrium properties for a square-well (SW) fluid confined to a slit-like pore employing canonical ensemble computer simulations. We compare our results for Π with those obtained indirectly by means of integration of the appropriate Gibbs-Duhem equation in conjunction with simulation results for

$\beta\mu^e$ (where $\beta = 1/kT$, k is Boltmann's constant and T the absolute temperature, and μ^e is the excess chemical potential per particle).

Π and $\beta\mu^e$ are calculated using special cases of a general method derived herein for numerically calculating an arbitrary first derivative of the canonical ensemble partition function with resepct to a simulation parameter. This method, which we call the *Virtual-Parameter-Variation* (VPV) method, has two special cases which have been employed in previous simulation methodology. One is the Widom test-particle-insertion (TPI) method[17] for calculating $\beta\mu^e$, and the other is a method for calculating pressure due originally to Eppenga and Frenkel[18], and also considered recently by Harismiadis *et. al.*[19]. Our method of calculating Π is a variant of these latter approaches.

In the next section of this paper, we derive the basis of the VPV method. In the subsequent section, we show results for bulk SW fluids as a test of the methodology. In the next section, we report new results for Π and for the phase equilibrium properties of square-well fluids confined to a slit-like pore. This is followed by conclusions.

2 The Virtual-Parameter-Variation (VPV) Method

From the standard expressions

$$d\beta A^e = U^e d\beta - \beta P^e dV + \beta\mu^e dN \quad (1)$$

$$\beta A^e = -\ln Q_N \quad (2)$$

where superscript e denotes an excess quantity above the ideal-gas value, A is the Helmholtz energy, U the internal energy, and Q_N is the canonical ensemble configurational partition function, it is formally seen that the derivatives of -ln Q_N with respect to a parameter x selected from the set $\{\beta, V, N\}$ are the respective coefficients of the differentials in eqn. (1). Other potential derivatives of interest might involve parameters related to the intermolecular pair potential, $u(12)$.

The TPI method[17] calculates $\beta\mu^e$ by performing trial particle insertions to calculate the

derivative $(\partial\beta A^e/\partial N)_{V,T}$. Similarly, although the pressure can be calculated in a standard way from the virial[20], it may also be calculated directly in the simulation by performing trial volume changes to compute $(\partial\beta A^e/\partial V)_{T,N}$. Thus, some time ago, Eppenga and Frenkel[18] developed a method for calculating the pressure of a hard platelet model system using this approach; for the complex geometry of this particular molecular model, the approach was computationally more efficient than using the virial. Recently, Harismiadis *et. al.*[19] generalized this approach to the calculation of the pressure for general intermolecular potential models, and applied it to the calculation of the pressure in Gibbs ensemble simulations. In the following, we derive a general method for calculating a first derivative of βA^e, which yields the two previously mentioned derivatives as special cases.

Consider a system being simulated in the (N, V, T) ensemble as the *reference system*, denoted by the subscript 0. Then we have

$$\exp(-\beta A_0^e) = Q_0 \tag{3}$$

where Q_0 is the partition function for the system with parameter value x_0. Changing x to give a new system labelled by the subscript 1, we have

$$\exp(-\beta A_1^e) = Q_1 \tag{4}$$

Dividing these two expressions yields

$$\exp(-\Delta\beta A^e) =< \exp(-\beta\Delta\mathcal{U}) >_0 \tag{5}$$

where Δ denotes a difference between quantities in systems 1 and 0, and $< ... >_0$ denotes a canonical ensemble average over configurations of the reference system. Setting

$$\Delta\beta A^e = \left(\frac{\partial\beta A^e}{\partial x}\right)\Delta x + O(\Delta x)^2 \tag{6}$$

and taking the limit $\Delta x \to 0$ and using equation (6) gives

$$\left(\frac{\partial\beta A^e}{\partial x}\right) = -\lim_{\Delta x\to 0}\frac{\ln < \exp(-\beta\Delta\mathcal{U}) >_0}{\Delta x} \tag{7}$$

Equation (7) is the basis of the Virtual-Parameter-Variation method.

We note that[21], if x and $\partial\beta A/\partial x$ form a conjugate intensive-extensive variable pair, one may perform computer simulations at fixed values of either quantity by means of a Legendre transformation. One example of such a variable pair for the canonical ensemble variables $\{N, V, \beta\}$ with thermodynamic potential βA is $\{N, \beta\mu\}$. Thus, $\beta\mu$ may be measured in a (N, V, β) (canonical ensemble) simulation using the TPI (which we would denote as VNV) method, which is a special case of equation (7). Correspondingly, grand canonical ensemble simulations correspond to fixed $\beta\mu \equiv \partial(\beta A)/\partial N$. Similarly, P may be measured in a canonical ensemble simulation using equation (7) (the VVV method), and (N, P, T) simulations correspond to fixed $\beta P \equiv -\partial\beta A/\partial V$. A third conjugate pair of variables is $\{\beta U, \beta\}$. As for the case considered by Eppenga and Frenkel[18], equation (7) may provide a convenient method to measure $\beta U \equiv \partial\beta A/\partial\beta$ in a computer simulation for systems of complex geometry. Finally, simulations at fixed βU may be implemented in an analogous manner. In all these cases, the simulations at specified values of $\beta\mu$, P, or U may be performed in a canonical ensemble using fluctuating values of V, N, or β, respectively. The transition probability for consecutive configurations is given by min (1, $\mathcal{P}_{\Delta x}$), where

$$\mathcal{P}_{\Delta x} = \exp\left(\frac{\partial\beta A^e}{\partial x}\Delta x - \beta\Delta\mathcal{U}\right) \tag{8}$$

This is a simple rearrangement of equation (7).

3 Models Studied and Computer Implementation Methodology

We implementated the VVV method to calculate the pressure and VNV (TPI) method to calculate $\beta\mu^e$ for model fluid systems consisting of square-well (SW) fluids, with intermolecular pair potential, $u(r)$, of the particles given by

$$u_{SW}(r_{12}) = \infty,\ r_{12} < \sigma \tag{9}$$

$$= -\epsilon,\ \sigma < r_{12} < \lambda\sigma \tag{10}$$

$$= \ 0, \ r_{12} > \lambda\sigma \tag{11}$$

where r_{12} is the distance between particles 1 and 2, σ is the hard-core diameter, ϵ is an energy parameter, and λ is the square-well width parameter (we used $\lambda = 1.5$ in our our calculations). In some cases, we also considered calculations for the hard-sphere (HS) fluid, for which the intermolecular potential is that of the SW fluid with $\lambda = 0$. We considered both bulk fluids and fluids confined to a slit pore characterized by hard walls separated by a distance L.

We performed conventional (N, V, T) simulations using 200 to 600 particles over a range of densities $\rho = N/V$ and temperatures, during the course of which we performed virtual volume change steps to calculate the pressure, and virtual particle insertions to calculate the excess chemical potential, $\beta\mu^e$.

For comparison purposes, for some bulk fluid simulations we also calculated the pressure using three additional routes. First, we used the virial equation pressure (denoted by P_{pdf}):

$$\frac{\beta P_{HS}}{\rho} = 1 + \frac{2}{3}\pi\rho\sigma^3 g_{HS}(\sigma) \tag{12}$$

$$\frac{\beta P_{SW}}{\rho} = 1 + \frac{2}{3}\pi\rho\sigma^3 \left\{ g_{SW}(\sigma) - \lambda^3 \left[g_{SW}(\lambda\sigma^-) - g_{SW}(\lambda\sigma^+) \right] \right\} \tag{13}$$

Second, we carried out (N, P, T) simulations using similar particle number and temperature ranges to those used in the (N, V, T) simulations. Third, we calculated the pressure by an indirect route (denoted by P_{GD}), numerically integrating $\beta\mu^e$ using the Gibbs-Duhem equation:

$$\beta P = \beta P^{ideal} + \beta P^e \tag{14}$$

$$= \rho + \rho\beta\mu^e - \int_0^\rho \beta\mu^e d\rho \tag{15}$$

For the slit fluid, we calculated the spreading pressure by the VVV method, (denoted by Π_{VVV}), and the excess chemical potential by the VNV method. We also calculated the pressure indirectly by integration of the Gibbs-Duhem equation to give

$$\beta\Pi = \beta\Pi^{ideal} + \beta\Pi^e$$

$$= \quad \rho + \rho\beta\mu^e - \int_0^\rho \beta\mu^e d\rho \tag{16}$$

We performed NPT, VNV (TPI), and Gibbs Ensemble[16] according to the standard methodology[20].

The VVV calculations for the slit fluid to calculate $\beta\Pi^e \equiv -(\partial\beta A^e/\partial V)_{N,\beta}$ were carried out as follows: We performed a conventional (N, V, T) simulation in a simulation box of cross-sectional area A with lengths $\ell_x = \ell_y \equiv \ell_{xy}$ in the x- and y-directions, and of height L corresponding to the wall separation distance of the slit. We employed the usual periodic boundary conditions in the x and y directions, accompanied by trial volume change steps conducted at appropriate intervals in the Markov chain of configurations. Each such step consisted of the following parts:

1. a random decrease of the simulation box volume $\Delta V = A\Delta\ell$, performed by a change of the length of the simulation box from l to $l - \Delta\ell$, where $\Delta\ell = \alpha\Delta\ell_{max}$, and α is a random number uniformly distributed on $[0, 1]$.

2. calculation of the resulting change in the Boltzmann factor, $\exp(-\beta\Delta\mathcal{U})$, where $\Delta\mathcal{U}$ is the change in the configurational energy $\mathcal{U}$ due to the volume change ΔV.

3. recording of the values of $\exp(-\beta\Delta\mathcal{U})$ in equal-sized bins of a volume histogram corresponding to ΔV in step 1.

At the end of the simulation run, the average values of $\exp(-\beta\Delta\mathcal{U})$ were analyzed as a function of ΔV, and extrapolated to $\Delta V = 0$. We did this by performing a linear regression of $\exp(-\beta\Delta\mathcal{U})$ on ΔV near $\Delta V = 0$.

For VVV calculations in a bulk fluid, there are several ways to perform the virtual volume changes of part 1 above. Due to the spatial isotropy, the volume changes may be effected by simultaneous alteration of the lengths of one or more of the three axes (ℓ_x, ℓ_y, ℓ_z) of the cubic simulation box. In order to calculate the spreading pressure, the relevant VVV-step requires random changes of the basic length ℓ_{xy}, where again a simultaneous alteration in either or

both the x- and y-directions may be performed. Based on careful examination of different strategies, the results reported in this paper were performed by changing the length of one axis of the simulation box only.

The Markov chains of the (N, V, T) simulations were constructed by sequences consisting of N one-particle translation moves. Following each N moves, we performed approximately $4N$ VVV or $10N$ VNV steps. In our simulations, a total number of between 5 and 20 million configurations per state point were generated.

For our calculations using equations (15) and (16), we first smoothed the simulation values of $\beta\mu^e$ using the software package TableCurve2D[22].

4 Bulk Fluid Results

We implemented the VVV method for the bulk fluid in order to verify the methodology. We calculated the derivative in eq. (7) by a numerical extrapolation procedure. We note that Harismiadis *et. al.*[19] calculated the pressure using a single small value of ΔV in the course of their simulations. Also, both Eppenga and Frenkel[18] and Harismiadis *et. al.*[19] calculated the system pressure by an analogue of equation (7). Since the ideal contribution to the pressure is known exactly, equation (7) should provide more accurate values of P.

A typical dependence of the quantity $\ln < \exp(-\beta\Delta\mathcal{U} >_0$ on ΔV in eq. (7) is shown in Fig. 1 for a subcritical temperature for the bulk SW fluid at a moderately high density. It is seen that the dependence is essentially linear, making the extrapolation to zero ΔV very precise. We performed linear regressions of $\ln < \exp(-\beta\Delta\mathcal{U} >_0$ on ΔV over several ranges of ΔV to obtain the slope of the line.

Fig. 2 shows the results for the total chemical potential $\beta\mu$, given by

$$\beta\mu = \ln(\rho\sigma^3) + \beta\mu^e \tag{17}$$

for a bulk SW fluid as a function of density for several isotherms. The van der Waals loops in the metastable and unstable regions are clearly evident. We generally found our simulation

results to be relatively insensitive to the simulation parameters (system size, equilibration strategy, and length of the simulations), even in the thermodynamically unstable vapor-liquid region.

Fig. 3 shows values of the pressure for the bulk SW fluid at the subcritical temperature $T^* \equiv kT/\epsilon = 1.05$ calculated using the VVV method, where they are compared with pressures obtained by alternative routes. We also show the HS results for comparison purposes, obtained from the analytical Carnahan-Starling-Kolafa equation of state[23]. The open circles indicate our VVV results. The inverted triangles are results obtained by us using NPT simulations, and the inverted triangles were obtained by us by means of NVT simulations and the virial equation of state, equation (13). The filled squares are phase coexistence results from the Gibbs Ensemble simulations of Vega *et. al* [25]. For the square-well fluid, the smoothed curves, corresponding to P_{GD}, were obtained from numerical integration of the smoothed chemical potential data of Fig. 2, using eqn. (15). The agreement of all the results is seen to be excellent.

We note that P_{GD} requires integration of the chemical potential results through the two-phase region of Fig. 2. The agreement of P_{GD} with the independently calculated simulation results is an indication that utilizing the chemical potential in this region provides a consistent route to calculating the pressure. Furthermore, the agreement of the P_{GD} and P_{VVV} in the two-phase region indicates the mutual consistency of the two approaches.

As a final test of the methodology for the bulk square-well bulk fluid, we calculated the phase equilibria and the critical point of the bulk SW fluid. For a given isotherm, using the smoothed $\beta\mu^e$ data, we numerically implemented the conditions of equal pressures and chemical potentials to solve for the coexistence densities and the vapor pressure. The results for three subcritical isotherms considered are shown in the upper portion of Table I, where they are compared with available simulation results. The indicated uncertainties for the Gibbs-Duhem (GD) pressures are a conservative estimate only, since they are very difficult to determine. The table shows that the GD results agree well with those of the simulations.

We calculated the critical point properties from our GD data by following the procedure of Vega *et. al.*[25], using a nonlinear regression procedure to fit the coexistence densities to the expression

$$\rho_{\ell/v} = \rho_c + C_2(1 - T/T_c) \pm 0.5B_0(1 - T/T_c)^{\beta};\ T < T_c \tag{18}$$

where ℓ and v denote respectively the liquid and vapor phases, T_c and ρ_c are the critical temperature and density respectively, and $\{C_2, B_0, \beta\}$ are constants. We subsequently estimated P_c by fitting the saturation pressures to the Antoine equation,

$$\ln P^* = A + B/T^* \tag{19}$$

where $P^* = P\sigma^3/\epsilon$, and using the calculated value of T_c^*. Our results are shown in the left portion of Table II, where they are compared with the corresponding results of Vega *et. al.*[25]. Uncertainties for our results were estimated by means of a sensitivity analysis of equations (18) and (19). The reasonable agreement of the calculated and simulation results in Tables I and II is an indication of the accuracy of the methodology we have used to estimate the phase equilibrium and critical properties.

5 Slit Fluid Results

Results for $\beta\mu$ as a function of density for the HS fluid confined to hard planar slits of various widths are shown in Fig. 4 (we also show the bulk-fluid HS results for comparison). The total chemical potential is calculated according to

$$\beta\mu = \ln(\rho_s\sigma^3) + \beta\mu^e \tag{20}$$

where $\beta\mu^e$ is the excess chemical potential per particle with respect to an ideal gas at the density ρ_s given by

$$\rho_s = \frac{N}{LA} \tag{21}$$

where A denotes an area parallel to the slit walls. The smoothed curve is a numerical fit to the simulation data. The results for the spreading pressure at several slit widths are shown in

Fig. 5. The curves were obtained by numerically integrating the smoothed chemical potential results of Fig. 4. As in the case of the bulk fluid, the agreement of Π_{GD} and Π_{VVV} is excellent.

Fig. 6 shows $\beta\mu$ for the square-well slit fluid as a function of density in a hard planar slit of width $L = 4\sigma$, at several temperatures. The smoothed curves are numerical fits to the simulation data, and the van der Waals loops indicate subcritical temperatures. Fig. 7 shows the spreading pressure calculated by the VVV method and by integration of the Gibbs-Duhem equation, (16), for systems of Fig. 6. As in the case of the bulk fluid, the agreement of Π_{VVV} with the Π_{GD} results is excellent, even in the two-phase region.

The phase equilibrium properties of the square-well slit fluid were estimated in the same way as that described for the bulk fluid case, and are given in Tables I and II. In Table I, it is seen that the phase equilibrium densities as predicted by means of the Gibbs-Duhem equation in conjunction with the smoothed $\beta\mu^e$ results agree well with the results obtained by means of the indicated corresponding Gibbs Ensemble simulation results, which we performed separately. For Table II, we used the phase equilibrium results of Table I at the three isotherms 0.90, 0.95. 1.00 in conjunction with equation (18) to estimate the critical point properties. It is seen that the critical temperature, pressure and density are all lower than in the case of the bulk fluid, as expected.

6 Conclusions

We have derived a general computer simulation method for numerically calculating an arbitrary first derivative of the canonical ensemble partition function with respect to a simulation parameter, which we call the Virtual-Parameter-Variation (VPV) method. Two special cases of this approach are the Widom test-particle insertion method[17] for calculating the excess chemical potential, $\beta\mu^e$ (which we call the VNV method), and a method of calculating pressure due originally to Eppenga and Frenkel[18] (which we call the VVV method).

We have used the VVV method to calculate the spreading pressure of model square-well fluids confined to a slit-like pore over a range of temperatures and densities. For each

isotherm, we have also calculated $\beta\mu^e$ by the VNV method, and obtained a corresponding thermodynamic pressure by integration of the Gibbs-Duhem equation. We have shown that the pressures calculated by these two routes are numerically consistent. We found that both the VNV method for $\beta\mu^e$ and the VVV method for the pressure can be used in a meaningful way within the thermodynamically unstable two-phase liquid-vapor region, both for bulk and confined fluids.

We have used the pressure results obtained from $\beta\mu^e$ and the Gibbs-Duhem equation to calculate the phase coexistence and critical properties of the bulk and confined fluids. We found the critical temperature of the confined fluid to be lower than that of the bulk fluid. Our results for the bulk case are in general agreement with those of other works. Our results in the case of square-well fluid confined to a hard planar slit are new.

7 Acknowledgement

This research was supported by NATO (Collaborative Research Grant No. CRG 972205), the National Research Council of Canada (Grant No. OGP 0001041), and the Deutsche Forschungsgemeinschaft (Sonderforschungsbereich 294).

Table 1: Phase equilibrium properties of the square-well fluid with $\lambda = 1.5$. $P^* = P\sigma^3/\epsilon, \Pi^* = \Pi\sigma^3/\epsilon, T^* = kT/\epsilon, \rho^* = N\sigma^3/V$ for the bulk fluid and $\rho^* = N\sigma A/L$ for the square-well fluid confined to a hard planar slit of width $L = 4\sigma$.

T^*	ρ_v^*		ρ_ℓ^*		P^*/Π^*	
	GD[a]	simulation	GD[a]	simulation	GD[a]	simulation
			Bulk			
0.90	0.013 ± 0.01	-	0.691 ± 0.01	-	0.010 ± 0.01	
1.05	0.043 ± 0.01	0.055 ± 0.003[b]	0.614 ± 0.01	0.634 ± 0.003[b]	0.034 ± 0.01	0.0430 ± 0.01[d]
		0.053 ± 0.002[c]		0.632 ± 0.007[c]		
1.20	0.142 ± 0.01	0.148 ± 0.008[b]	0.480 ± 0.01	0.445 ± 0.010[b]	0.084 ± 0.01	0.1035 ± 0.04[d]
		0.147 ± 0.017[c]		0.448 ± 0.040[c]		
			Slit, $L = 4\sigma$			
0.80	0.012 ± 0.01	0.012 ± 0.005[e]	0.525 ± 0.01	0.516 ± 0.015[e]	0.020	-
0.90	0.031 ± 0.01	0.0282 ± 0.005[e]	0.463 ± 0.01	0.450 ± 0.012[e]	0.020	-
0.95	0.049 ± 0.01	0.0546 ± 0.008[e]	0.429 ± 0.01	0.434 ± 0.012[e]	0.030	-
1.00	0.083 ± 0.01	-	0.380 ± 0.01	-	0.041	-

[a] results obtained by using the smoothed $\beta\mu^e$ simulation results in conjunction with the Gibbs-Duhem equation, (15) or (16)

[b] Gibbs Ensemble simulations of Smith and Vörtler[9]

[c] Gibbs Ensemble simulation results of Vega *et. al.*[25]

[d] average of vapor and liquid phase results of Vega *et. al.*[25]

[e] Gibbs Ensemble simulations, this work

[a] Gibbs Ensemble simulation results of Vega *et. al.*[25], $N = 512$ particles

[b] density scaling Monte Carlo results of Brilliantov and Valleau[26], $N = 256$

[c] density scaling Monte Carlo results of Brilliantov and Valleau[26], $N = \infty$

[d] grand canonical simulation results of Ourkoulas and Panagiotopoulos[27], $N = \infty$

[e] molecular dynamics results of Elliot and Hu[28], $N = 108$

Table 2: Critical properties of the square-well fluid with $\lambda = 1.5$ confined to a hard planar slit of width $L = 4\sigma$. GD denotes values calculated from the corresponding results of Table I. $\{\beta, B_0, C_2\}$ are the fitted parameters in equation (18). $Z = PV/NkT$ is the compressibility factor. A and B are the parameters of the Antoine equation, (19). See Table I for further notation.

	Bulk		Slit, $L = 4\sigma$
	GD	Simulation	GD
T_c^*	1.228 ± 0.012	1.219 ± 0.008[a]	1.034 ± 0.004
		1.246 ± 0.005[b]	
		1.22 ± 0.01[c]	
		1.218 ± 0.002[d]	
		1.27[e]	
P_c^*/Π_c^*	0.098 ± 0.06	0.108 ± 0.016[a]	0.051 ± 0.03
		0.1090 ± 0.001[b]	
		0.095 ± 0.001[d]	
		0.11[e]	
ρ_c^*	0.306 ± 0.005	0.299 ± 0.023[a]	0.226 ± 0.001
		0.329 ± 0.006[b]	
		0.310 ± 0.001[d]	
		0.306[e]	
Z_c	0.26 ± 0.03	0.30 ± 0.07[a]	0.22 ± 0.02
		0.252 ± 0.003[d]	
		0.30[e]	
β	0.28 ± 0.05	0.30 ± 0.02	0.27 ± 0.02
B_0	0.98 ± 0.06	1.04 ± 0.04	0.75 ± 0.02
C_2	.17 ± 0.03	0.27 ± 0.13	0.16 ± .01
A	3.83	3.67	3.37
B	-7.57	-7.19	-6.57

References

[1] D. Henderson, S. Sokolowski, and D. T. Wasan, J. Phys. Chem. **B102**, 3009 (1998).

[2] E. Kierlik, M. L. Rosinberg, G. Tarjus, and P. A. Monson, J. Chem. Phys. **106**, 264 (1997).

[3] W. Dong, E. Kierlik, and M. L. Rosinberg, Phys. Rev. **E50**, 4750 (1994).

[4] D. M. Ford and E. M. Glandt, Phys. Rev. **E50**, 1280 (1994).

[5] R. Pospisil, A. Malijevsky, P. Jech, and W. R. Smith, Molec. Phys., **78**, 1461 (1993).

[6] C. Vega, R. D. Kaminsky, and P. A. Monson, J. Chem. Phys. **99**, 3003 (1993).

[7] A. Z. Panagiotopoulos, Molec. Phys. **62**, 701 (1987).

[8] W. R. Smith, H. L. Vörtler, R. Kao, and I. Nezbeda, Paper #7l, Am. Inst. Chem. Eng. Annual Meeting, Miami Beach, Nov. 12-17, 1995.

[9] W. R. Smith and H. L. Vörtler Chem. Phys. Letters, **249**, 470 (1996).

[10] S. Labik and W. R. Smith, Molec. Phys. **88**, 1411, (1996).

[11] K. S. Page and P. A. Monson, Phys. Rev. **E54**, R29 (1996).

[12] J. Forsman and C. E. Woodward, Molec. Phys. **90**, 637 (1997).

[13] H. Dominguez, M. P. Allen and R. Evans, Molec. Phys. **96**, 209 (1999).

[14] R. Evans, J. Phys. Conds. Matter **2**, 8989 (1990).

[15] D. M. Ruthven, *Principles of Adsorption and Adsorption Processes*, Wiley-Interscience, 1984.

[16] A. Z. Panagiotoupolos, Molec. Sim. **9**, 1 (1992).

[17] B. Widom, J. Chem. Phys. **39**, 2808 (1963).

[18] R. Eppenga and D. Frenkel, Molec. Phys. **52**, 52, 1303 (1984).

[19] V. I. Harismiadis, J. Vorholz and A. Z. Panagiotopoulos, Molec. Phys. **62**, 701 (1996).

[20] M. P. Allen and D. J. Tildesley, *Computer Simulation of Liquids*, Clarendon Press, Oxford (1987).

[21] A. Münster, *Statistical Thermodynamics, Vol, I*, Springer-Verlag, Berlin, 1969, Section 3.2.

[22] TableCurve 2D, Version 4, Jandel Scientific Software, 1996.

[23] T. Boublik and I. Nezbeda, Coll. Czechoslovak. Chem. Commun., **61**, 2301 (1986).

[24] Maple V, Version 5.00, Waterloo Maple Software, Inc., 1997.

[25] L. Vega, E. de Miguel, L. F. Rull, G. Jackson, and I. A. McLure, J. Chem. Phys. **96**, 2296 (1992).

[26] N. V. Brilliantov and J. P. Valleau, J. Chem. Phys, **108**, 1115 (1198); **108**, 1123 (1998).

[27] G. Ourkoulas and A. Z. Panagiotopoulos, J. Chem. Phys. **110**, 1581 (1999).

[28] J. R. Elliot and L. Hu, J. Chem. Phys., **110**, 3043, 1999.

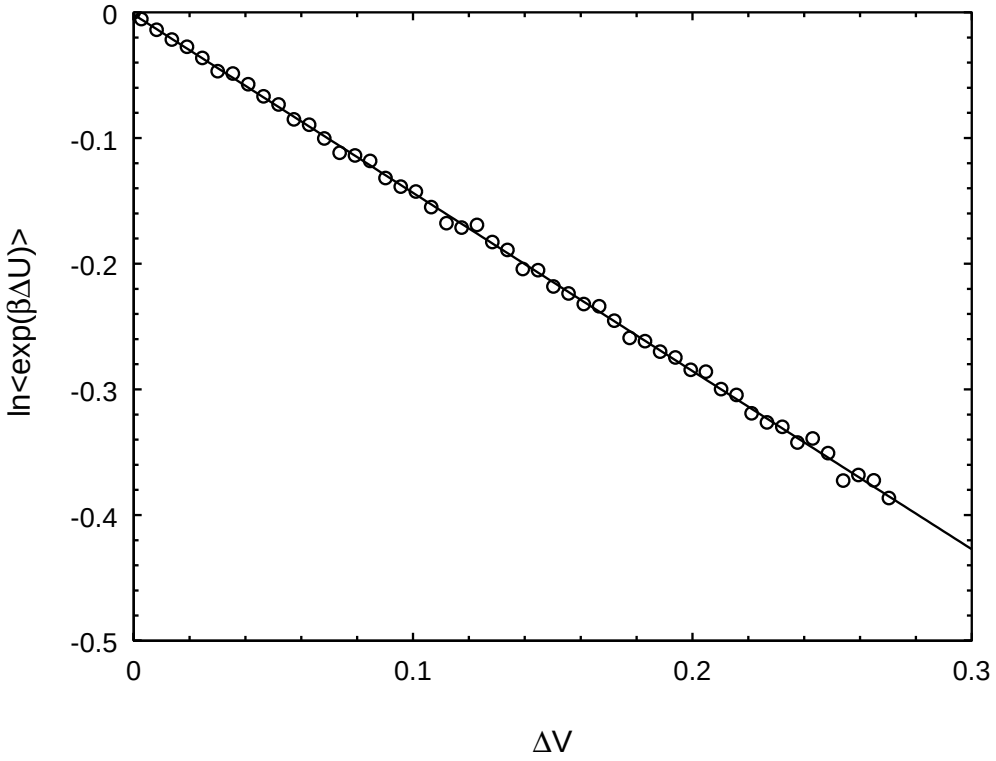

Figure 1: Illustrative calculation of P^e_{VVV} by extrapolating the ratio in equation (7) to $\Delta V = 0$ (solid line), where ΔV is the trial volume change. The circles are the raw simulation data. The results shown are for a bulk square-well fluid with λ=1.5 at the state point $T^* = 1.05,\ \rho\sigma^3 = 0.7909$.

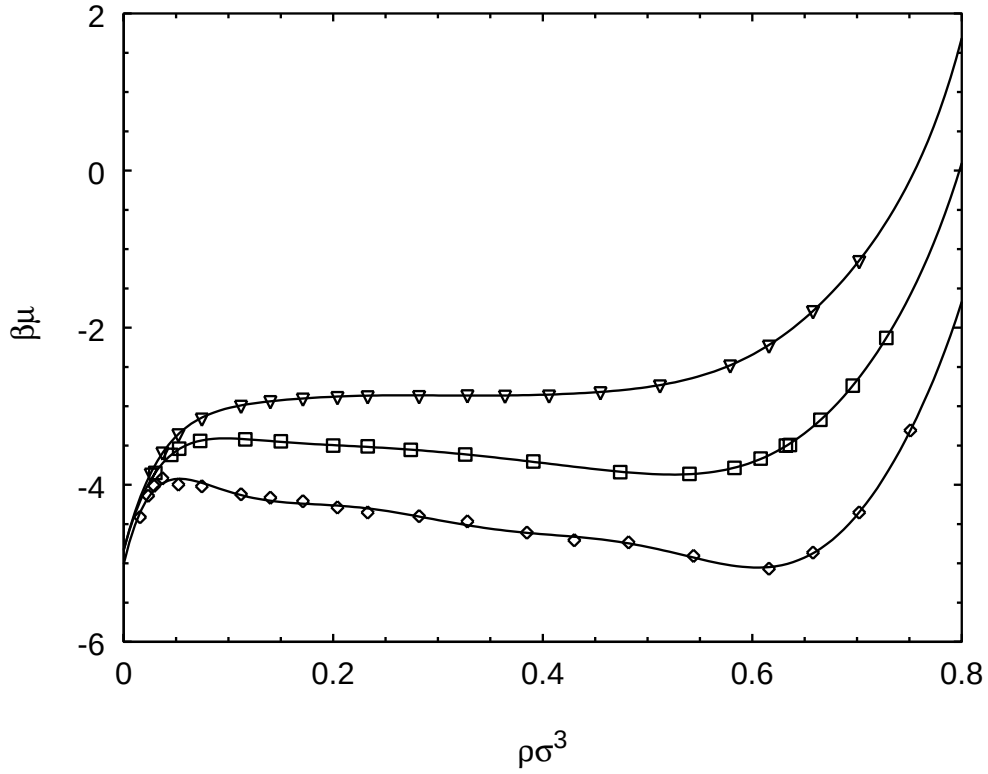

Figure 2: Total chemical potential, $\beta\mu$, of the bulk square-well (SW) fluid with $\lambda = 1.5\sigma$ as a function of density, calculated using the TPI method. Several isotherms are shown; the curves are smoothed numerical fits to the computer simulation data. Circles denote results at $T^* = 0.90$; squares, $T^* = kT/\epsilon = 1.05$; and inverted triangles, $T^* = 1.25$.

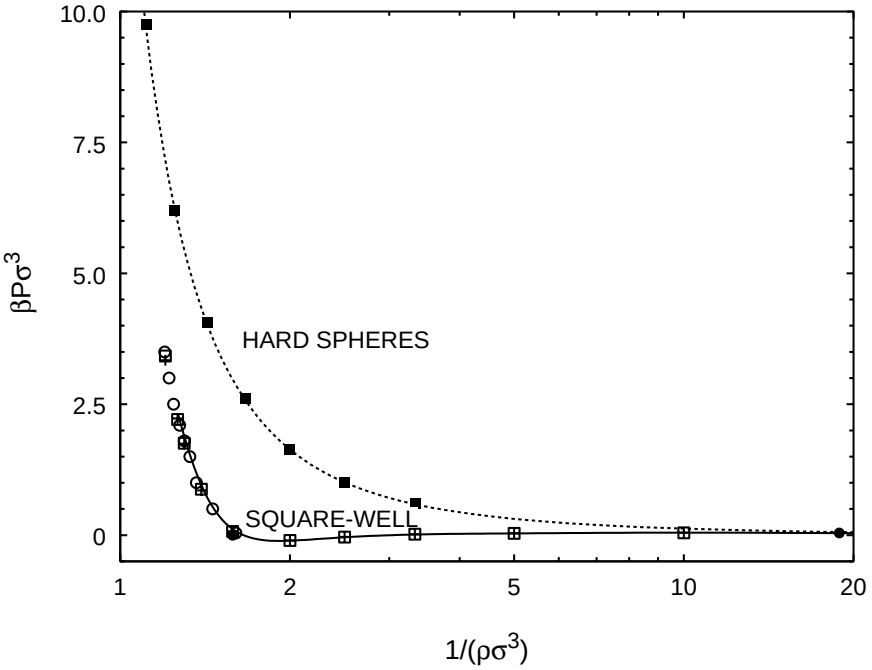

Figure 3: Pressure of the bulk hard-sphere (HS) and of a square-well (SW) fluid with $\lambda = 1.5\sigma$, as a function of reduced volume. The SW fluid is at the reduced temperature $T^* = 1.05$. The curve for the HS fluid is the result of the analytical Carnahan-Starling-Kolafa equation of state[23]; for the SW fluid, the curve is result of the Gibbs-Duhem equation, (15), using the smoothed chemical potential data of Figure 2. Squares are the VVV results, open circles are N, P, T simulation results, crosses are the results of the virial equation, (13), and filled circles are the liquid-vapor coexistence results of Vega *et. al.*.[25]

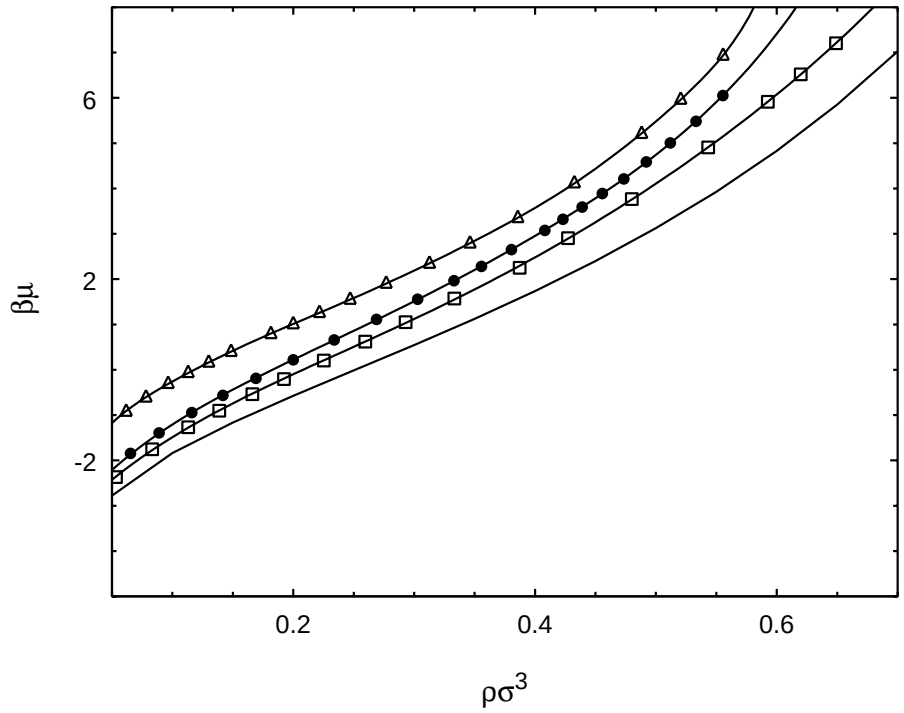

Figure 4: Total chemical potential of the hard-sphere fluid in a hard planar slit as a function of density for several slit widths, calculated using the TPI method. The curves are smoothed numerical fits to the computer simulation data. Also shown (lower curve, for comparison only) are the hard-sphere bulk-fluid results, obtained from the analytical Carnahan-Starling-Kolafa equation of state[23]. The triangles denote results at the slit width $L = 1.25\sigma$; circles at $L = 2.5\sigma$; and squares at $L = 4\sigma$.

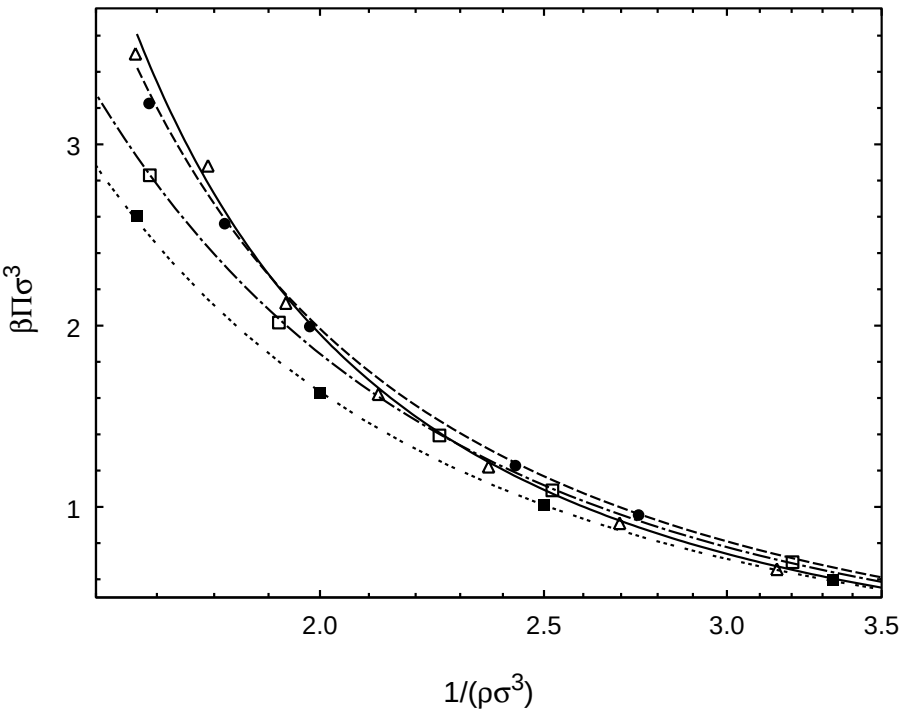

Figure 5: Spreading pressure of the hard-sphere fluid in a hard planar slit as a function of reduced volume for the slit widths shown in Fig. 4. The curves are the results of the Gibbs-Duhem equation, (16), using the smoothed chemical potential data of Fig. 4. The symbols denote the VVV results; for notation, see the caption to Fig. 4. The bulk fluid results are shown for comparison purposes; the dashed line is the result of the Carnahan-Starling-Kolafa equation of state[23] and the filled squares are the VVV results.

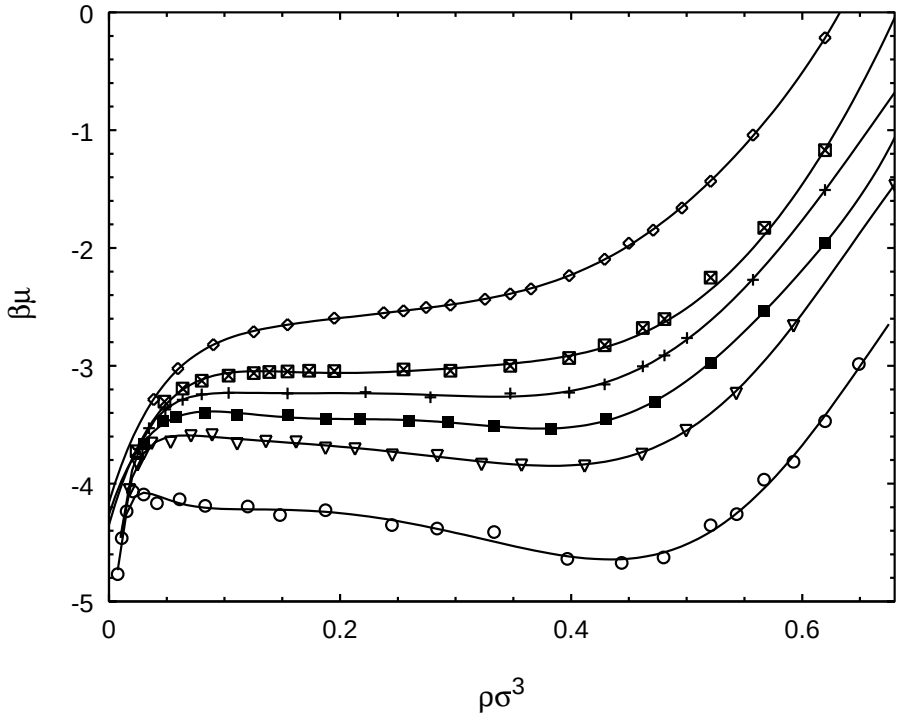

Figure 6: Total chemical potential of the square-well fluid with $\lambda = 1.5\sigma$ in a hard planar slit of width $L = 4\sigma$ as a function of density at several reduced temperatures, $T^* = kT/\epsilon$, calculated using the TPI method. The curves are smoothed numerical fits to the computer simulation data. Open circles denote results at $T^* = 0.8$, inverted triangles at $T^* = 0.9$, filled squares at $T^* = 0.95$, crosses at $T^* = 1.0$, crosses in squares at $T^* = 1.05$, and diamonds at $T^* = 1.2$.

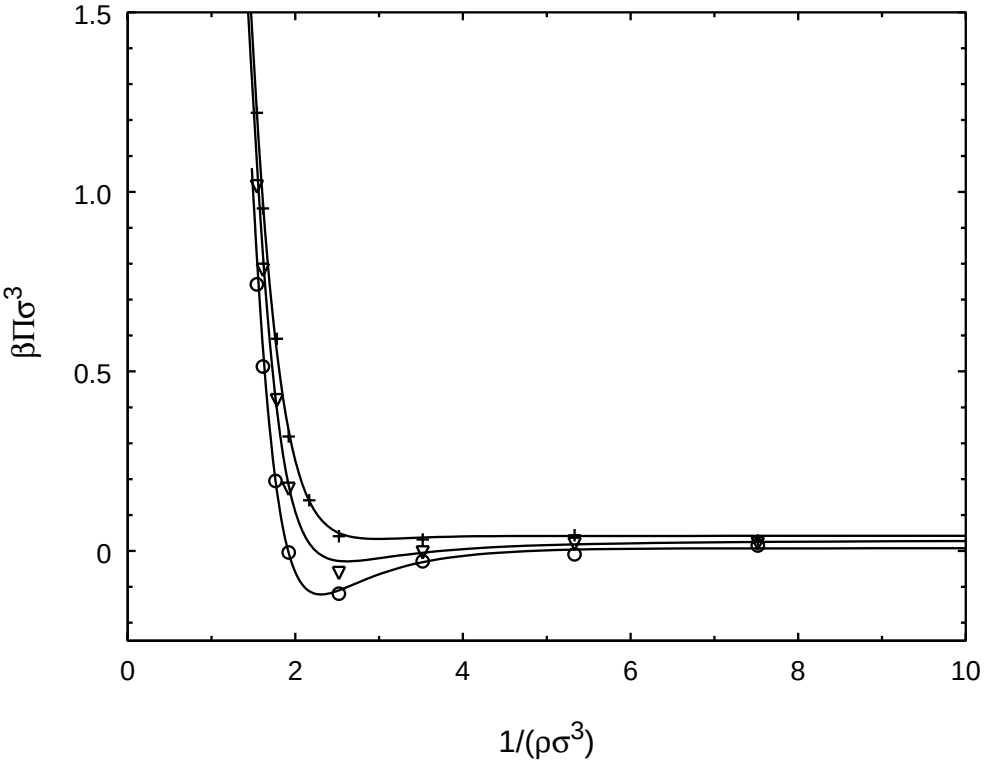

Figure 7: Spreading pressure of a square-well fluid with $\lambda = 1.5\sigma$ in a hard planar slit of width $L = 4\sigma$ as a function of reduced volume at the temperatures of Fig. 6. Symbols are the VVV results, and the curves are obtained from the Gibbs-Duhem equation, (16), using the smoothed chemical potential data of Fig. 6. See Fig. 6 for explanation of the symbols.

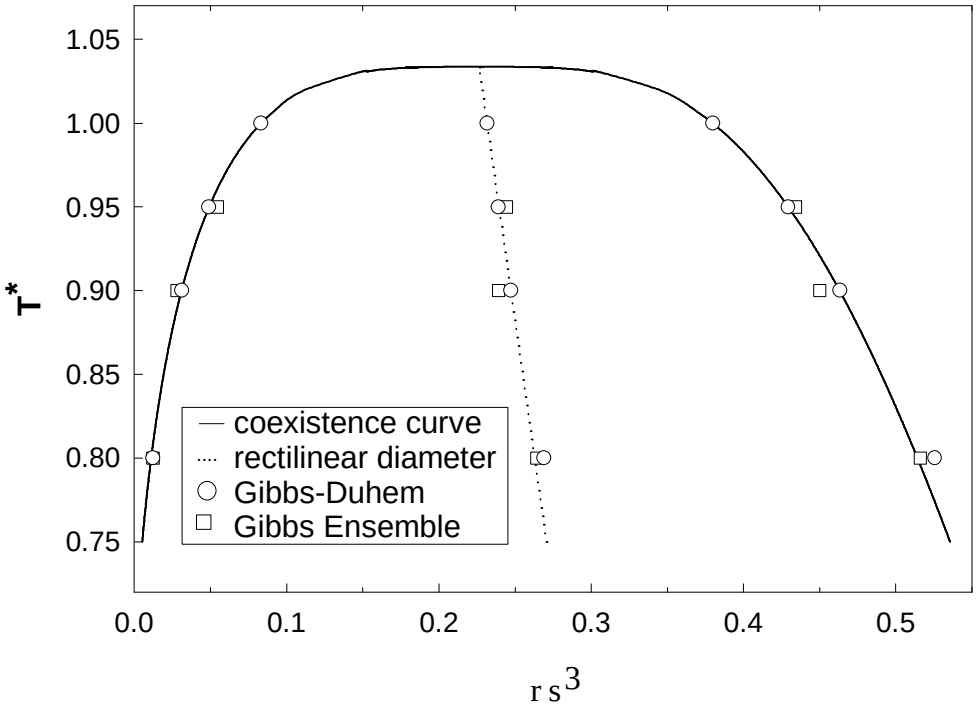

Figure 8: Temperature-density vapor-liquid coexistence curve (solid line) for the square-well fluid with $\lambda = 1.5$ in a hard planar slit of width $L = 4\sigma$. The rectilinear diameter line given by $(\rho_\ell + \rho_v)/2$ is also shown (dotted line). The curves are the result of a numerical fit to equation (18); circles are the phase equilibrium data from Table I, and squares are the Gibbs Ensemble simulation results from Table I.